



Real-time optimization of wind farms using modifier adaptation and machine learning

Leif Erik Andersson¹ and Lars Imsland¹

¹Norwegian University of Science and Technology, Department of Engineering Cybernetics, 7491 Trondheim, Norway

Correspondence: Leif Erik Andersson (leif.e.andersson@ntnu.no)

Abstract. Real-time optimization (RTO) covers a family of optimization methods that incorporate process measurements in the optimization to drive the real process (plant) to optimal performance while guaranteeing constraint satisfaction. Modifier Adaptation (MA) introduces zeroth and first-order correction terms (bias and gradients) for the cost and constraint functions. Instead of updating the plant model, in MA the optimization problem is updated directly from data **guaranteeing to meet the necessary condition of optimality upon convergence.**

5

The main burden of the MA approach is **the estimation of the first-order modifiers of the cost and constraint functions at each RTO iteration.** Finite-difference approximation is the most common approach that requires **at least $n_u + 1$ steady-state operation points to estimate the gradients,** where n_u is the number of control inputs. Obtaining these **can require a long convergence time.** For this reason, this work considers the use of Gaussian process (GP) regression to estimate the plant-model mismatch based on plant measurements, and replace the usual modifiers by these high order regression functions. GP is a probabilistic, non-parametric modelling technique well known in the machine learning community. The approach is tested on several numerical test cases simulating wind farms. It is shown that the approach is able to correct the model and **converges to the plant optimal point.** Several improvements for large inputs spaces, which is a challenging problem for the approach presented in the article, are discussed.

10

15 1 Introduction

Currently the wind turbines in a wind farm are operated at their **individual optimal operating point.** This control strategy is called *greedy* wind farm control since the interactions between turbines are not taken into account. However, it is expected that the greedy control strategy leads to **sub-optimal** performance of the wind farm (Steinbuch et al., 1988; Johnson and Thomas, 2009; Barthelmie et al., 2009). A coordinated wind farm controller, which takes the wake interactions between turbines in a wind farm into account, may result in a **superior performance** compared to the greedy wind farm controller. The two main wind farm control strategies are axial induction control, e.g. Steinbuch et al. (1988); Corten and Schaak (2003); Horvat et al. (2012); Rotea (2014); Munters and Meyers (2016) and wake steering control, e.g. Medici (2005); Adaramola and Krogstad (2011); Wagenaar et al. (2012); Park et al. (2013); Gebraad and Van Wingerden (2014). The idea behind the former is to deviate the blade pitch and generator torque of the upwind turbine from the greedy control settings. As a consequence, the velocity deficit in the wake behind the turbine and **the power production of the downwind turbine changes.** The target net effect is an overall

20

25





increase of the power production and possibly an decrease of fatigue loads. However, recent studies suggest that axial induction control using steady-state models to calculate the optimal control settings may be unable to improve the power production of a wind farm (Schepers and Van der Pijl, 2007; Campagnolo et al., 2016; Bartl and Sætran, 2016; Annoni et al., 2016) 

The currently more promising wind farm control strategy using steady-state models is wake steering. The goal of wake steering is to deflect the wake away from the downwind turbine by using the yaw settings of the upwind turbine. Field experiments showing promising results were conducted by Fleming et al. (2017, 2019); Howland et al. (2019). In these experiments lookup tables with optimal yaw settings of each turbine are created with help of an steady-state model. Hence the wind farm is operated in an open-loop control setting.

The steady-state wake models used in model-based control are usually relatively simple. They estimate the velocity deficit in wakes. For a long time one of the most popular wake models was the Jensen Park model (Jensen, 1983; Katic et al., 1987). Jiménez et al. (2010) developed one of the first steady-state wake models that described wake deflection due to yaw. A recent wake model, which is also used in this study, was presented by Bastankhah and Porté-Agel (2016). It is based on mass and momentum conservation and assumes a Gaussian distribution of the velocity deficit in the wake. The steady-state wake models are able to describe the general behaviour of the wake (Barthelmie et al., 2013; Annoni et al., 2014). Nevertheless, they are just vague approximations of a complex phenomena that is, in fact, not well understood (Veers et al., 2019). Hence, real time optimization (RTO), which incorporates plant measurements to improve the performance of the wind farm controller, is extremely useful for this process.

Probably one of the most intuitive RTO strategies is the "two-step" approach. Here, first the model parameters are updated, and then new control inputs are computed based on the updated model. The two steps refer to the parameter optimization and control input optimization, which are performed sequentially (Marchetti et al., 2016). However, the two-step approach cannot guarantee plant optimality upon convergence if the model is structurally incorrect (Marchetti et al., 2016). An example that an improved parameterisation of the steady-state wake model was not able to remove the mismatch between a low order model and a high fidelity model of wake is given in Fleming et al. (2018).

In contrast, modifier adaptation (MA) corrects the cost and constraint functions of the optimization problem directly, and reaches, under suitable assumptions, true plant optimality upon convergence (Marchetti et al., 2009). The bottleneck of the MA approach is the estimation of the gradients of the objective and constraint functions at each RTO iteration. Finite difference approximation is one of the most common approaches that requires $n_u + 1$ steady-state operation points to estimate the gradients, where n_u is the amount of control inputs. These can lead to a long convergence time, especially for processes with high dimensional input spaces. Therefore, in this work Gaussian process (GP) regression is combined with MA (de Avila Ferreira et al., 2018; del Rio Chanona et al., 2019). GP is a probabilistic, non-parametric modelling technique well known in the machine learning community (Rasmussen and Williams, 2006). The GP regression model estimates the plant-model mismatch using plant measurements. Then the GP model is used to correct the original optimization problem and by this improve the optimization of the plant inputs. 

The article is structured as follows: In Section 2 the optimization problem is formulated and Gaussian process regression is explained. In Section 3 the modifier adaptation using Gaussian process regression is presented and the numerical turbine



and wake models introduced. The approach is tested numerically ~~on several examples~~ in Section 4. The article ends with a conclusion.

2 Problem formulation

The optimization problem of the steady-state plant performance subject to constraints can be formulated as (Marchetti et al., 2016):

$$\mathbf{u}_p^* = \arg \min_{\mathbf{u}} \phi_p(\mathbf{u}, \mathbf{y}_p(\mathbf{u})) \quad (1a)$$

$$s.t. \ G_{p,j}(\mathbf{u}) := g_{p,j}(\mathbf{u}, \mathbf{y}_p(\mathbf{u})) \leq 0, \ j = 1, \dots, n_g, \quad (1b)$$

$$\mathbf{u} \in \mathcal{U}, \quad (1c)$$

where $\mathbf{u} \in \mathbb{R}^{n_u}$ and $\mathbf{y}_p \in \mathbb{R}^{n_y}$ denote the plant input and output variables, respectively; $\mathbf{u} \in \mathbb{R}^{n_u}$ and $\mathbf{y}_p \in \mathbb{R}^{n_y}$ are the input-output pairs of the wind farm; $\phi_p: \mathbb{R}^{n_u} \rightarrow \mathbb{R}$ is the cost function to be minimized; $g_{p,j}: \mathbb{R}^{n_u} \times \mathbb{R}^{n_y} \rightarrow \mathbb{R}$, $j = 1, \dots, n_g$, are the inequality constraint functions; and $\mathcal{U} \subseteq \mathbb{R}^{n_u}$ is the control domain, e.g. box constraints on the control inputs. Formulation (1) assumes that ϕ_p and $g_{p,j}$ as functions of \mathbf{u} , and \mathbf{y}_p are exactly known. However, in any practical application the exact input-output map of the plant is unknown and instead an approximate model of the system is exploited for the optimization:

$$\mathbf{u}^* = \arg \min_{\mathbf{u}} \phi(\mathbf{u}, \mathbf{y}(\mathbf{u})) \quad (2a)$$

$$s.t. \ G_j(\mathbf{u}) := g_j(\mathbf{u}, \mathbf{y}(\mathbf{u})) \leq 0, \ j = 1, \dots, n_g, \quad (2b)$$

$$\mathbf{u} \in \mathcal{U}, \quad (2c)$$

where the quantities ϕ , $g_j(\mathbf{u}, \mathbf{y}(\mathbf{u}))$, \mathbf{u}^* , and G_j refer to the inexact model counterparts of the true plant optimization problem in Eq. (1).

RTO takes advantage of the available measurements to compensate for plant-model mismatch and adapt the model-based optimization problem Eq. (2) to reach plant optimality.

The standard MA approach applies first-order correction terms that are added to the cost and constraint functions to match the necessary conditions of optimality upon convergence (Marchetti et al., 2009). Iteratively the following modified optimization problem is solved:

$$\hat{\mathbf{u}}_{k+1}^* = \arg \min_{\mathbf{u}} \phi(\mathbf{u}, \mathbf{y}(\mathbf{u})) + (\boldsymbol{\lambda}_k^\phi)^T \mathbf{u} \quad (3a)$$

$$s.t. \ G_j(\mathbf{u}) + \varepsilon_{j,k} + (\boldsymbol{\lambda}_k^{G_j})^T (\mathbf{u} - \mathbf{u}_k) \leq 0, \ j = 1, \dots, n_g, \quad (3b)$$

$$\mathbf{u} \in \mathcal{U}, \quad (3c)$$



where $\hat{\mathbf{u}}_{k+1}^*$ is the optimal solution at iteration $k+1$, the $\varepsilon_{j,k} \in \mathbb{R}$ are the zeroth-order modifiers for the constraints, and λ_k^ϕ and $\lambda_k^{G_j}$ are the first-order modifiers for the cost and constraints, respectively. The correction terms are given by:

$$\varepsilon_{j,k} := G_{p,j}(\mathbf{u}_k) - G_j(\mathbf{u}_k), \quad (4a)$$

$$90 \quad (\lambda_k^\phi)^T := \frac{\partial \phi_p}{\partial \mathbf{u}}(\mathbf{u}_k) - \frac{\partial \phi}{\partial \mathbf{u}}(\mathbf{u}_k), \quad (4b)$$

$$(\lambda_k^{G_j})^T := \frac{\partial G_{p,j}}{\partial \mathbf{u}}(\mathbf{u}_k) - \frac{\partial G_j}{\partial \mathbf{u}}(\mathbf{u}_k). \quad (4c)$$

It is recommended to filter the input update $\hat{\mathbf{u}}_{k+1}^*$ to avoid excessive correction and reduce sensitivity to noise (Marchetti et al., 2016):

$$\mathbf{u}_{k+1} = \mathbf{u}_k + \mathbf{L}(\hat{\mathbf{u}}_{k+1}^* - \mathbf{u}_k), \quad (5)$$

95 with $\mathbf{L} = \text{diag}(l_1, \dots, l_{n_u})$, $l_i \in (0, 1]$ where l_i may be reduced to help stabilize the iterations.

The MA scheme requires the estimation of the plant gradients at each RTO iteration, which is experimentally expensive and the main bottleneck for MA implementation in practice (Marchetti et al., 2016).

2.1 Gaussian processes

100 In this section we give a brief outline of GP regression ~~for our purposes~~, for more information ~~refer to~~ Rasmussen and Williams (2006). GP regression aims to identify an unknown function $f: \mathbb{R}^{n_u} \rightarrow \mathbb{R}$ from data. Let the noisy observation of $f(\cdot)$ be given by:

$$y_k = f(\mathbf{u}_k) + \nu_k \quad (6)$$

where the value $f(\cdot)$ is perturbed by Gaussian noise ν_k with zero mean and variance σ_ν^2 , $\nu_k \sim \mathcal{N}(0, \sigma_\nu^2)$.

105 We assume $f(\cdot)$ to follow a GP with a zero mean function and the squared-exponential (SE) covariance function. The choice of the mean and covariance functions ~~assume certain smoothness and continuity properties of the underlying function~~ (Snelson and Ghahramani, 2006). The SE covariance function can be expressed as follows:

$$k(\mathbf{u}_i, \mathbf{u}_j) = \sigma_f^2 \exp\left(-\frac{1}{2}(\mathbf{u}_i - \mathbf{u}_j)^T \mathbf{\Lambda}^{-1}(\mathbf{u}_i - \mathbf{u}_j)\right) \quad (7)$$

where σ_f^2 is the covariance magnitude and $\mathbf{\Lambda} = \text{diag}(\lambda_1^2, \dots, \lambda_{n_u}^2)$ is a scaling matrix.

110 Assume we are given a training dataset $\mathcal{D} = \{\mathbf{U}, \mathbf{Y}\}$ of size M consisting of M input vectors $\mathbf{U} = [\mathbf{u}_1, \dots, \mathbf{u}_M]^T$ and corresponding observations $\mathbf{y} = [y_1, \dots, y_M]^T$ according to Eq. (6). From ~~the GP distribution the data~~ then follows a joint multivariate Gaussian distribution, which can be stated as:

$$p(\mathbf{y}|\mathbf{U}) = \mathcal{N}(\mathbf{0}, \mathbf{K} + \sigma_\nu^2 \mathbf{I}) \quad K_{ij} = k(\mathbf{u}_i, \mathbf{u}_j) \quad (8)$$

The hyperparameters $\psi := [\sigma_f, \sigma_\nu, \lambda_1, \dots, \lambda_{n_u}]^T$ are commonly unknown and hence need to be inferred from data. ~~In this article the log marginal likelihood $p(\mathbf{y}|\mathbf{U})$ is used.~~ Ignoring constant terms and factors, this can be stated as:

$$115 \quad \mathcal{L}(\mathcal{D}, \Psi) = -\frac{1}{2} \mathbf{y}^T (\mathbf{K} + \sigma_\nu^2 \mathbf{I})^{-1} \mathbf{y} - \frac{1}{2} \ln |\mathbf{K} + \sigma_\nu^2 \mathbf{I}|. \quad (9)$$





The required maximum likelihood estimate is then given by $\hat{\psi} \in \arg \max_{\psi} \mathcal{L}(\mathcal{D}, \psi)$.

Next we require the predictive distribution of $f(\mathbf{u})$ at an arbitrary input \mathbf{u} , which can be found by the conditional distribution of $f(\mathbf{u})$ on the data distribution $p(\mathbf{y}|\mathbf{U})$. From the GP assumption this has a closed-form solution and can be stated as:

$$f(\mathbf{u})|\mathcal{D}, \hat{\psi} \sim \mathcal{N}(\mu_{\text{GP}}(\mathbf{u}; \mathcal{D}, \hat{\psi}), \sigma_{\text{GP}}^2(\mathbf{u}; \mathcal{D}, \hat{\psi})) \quad (10)$$

$$120 \quad \mu_{\text{GP}}(\mathbf{u}; \mathcal{D}, \hat{\psi}) = \mathbf{k}^T(\mathbf{u})(\mathbf{K} + \sigma_{\nu}^2 \mathbf{I})^{-1} \mathbf{y} \quad (11)$$

$$\sigma_{\text{GP}}^2(\mathbf{u}; \mathcal{D}, \hat{\psi}) = \sigma_f^2 - \mathbf{k}^T(\mathbf{u})(\mathbf{K} + \sigma_{\nu}^2 \mathbf{I})^{-1} \mathbf{k}(\mathbf{u}) \quad (12)$$

where $\mu_{\text{GP}}(\mathbf{u}; \mathcal{D}, \hat{\psi})$ can be seen as the GP prediction at \mathbf{u} and $\sigma_{\text{GP}}^2(\mathbf{u}; \mathcal{D}, \hat{\psi})$ as a corresponding measure of uncertainty to this prediction. The GP is a non-parametric model. The training data are explicitly required to construct the predictive distribution. For the above expression a matrix of size $M \times M$ must be inverted, which prohibits large data sets.

125 3 Methodology

3.1 Modifier Adaptation with Gaussian processes

The use of GPs in a MA approach to overcome the limitation of estimating the plant gradients was first proposed by de Avila Ferreira et al. (2018). The idea is to replace the zeroth- and first-order modifiers of the cost and constraints in (3) with GP regression terms. **Since the wind farms considered in this article do not have inequality constraint functions** they are not included in this section. However, inequality constraint functions can be easily incorporated into the method.

130

The training set of the GP to correct the objective function are the controlled inputs of the approximate model and the plant-model mismatch of the objective function. The new optimization problem of the MA scheme with GP modifiers (MA-GP) is

$$\hat{\mathbf{u}}_{k+1}^* = \arg \min_{\mathbf{u}} \phi(\mathbf{u}, \mathbf{y}(\mathbf{u})) + \mu_{\text{GP},k}^{\phi_p - \phi}(\mathbf{u}; \mathcal{D}_0, \hat{\psi}_0), \quad s.t. \quad \mathbf{u} \in \mathcal{U}, \quad (13)$$

135 where the plant-model mismatch of the cost function is modelled by $\mu_{\text{GP}}^{\phi_p - \phi}$. Similar to the original MA scheme the optimal input of Eq. (13) may be filtered with Eq. (5) to reduce the step-size and help stabilize the MA-GP scheme (del Rio Chanona et al., 2019). The whole MA-GP scheme is presented in Algorithm 1 and Fig. 1.

In Algorithm 1 the hyperparameters are updated if *HypOpt* is true. *HypOpt* is a user-defined condition, which allows to update the hyperparameter. The extrema are to update the hyperparameter each iteration or never. The hyperparameter update is usually the computational bottle-neck of the MA-GP algorithm. **Especially for large data sets it can be expected that the hyperparameter do not change much from one iteration to the next.** Therefore, it is reasonable  update the hyperparameters less frequent.

140

¹The wind farm picture is by Erik Wilde from Berkeley, CA, USA <https://www.flickr.com/photos/dret/24110028330/>, *Wind turbines in southern California 2016*, <https://creativecommons.org/licenses/by-sa/2.0/legalcode>

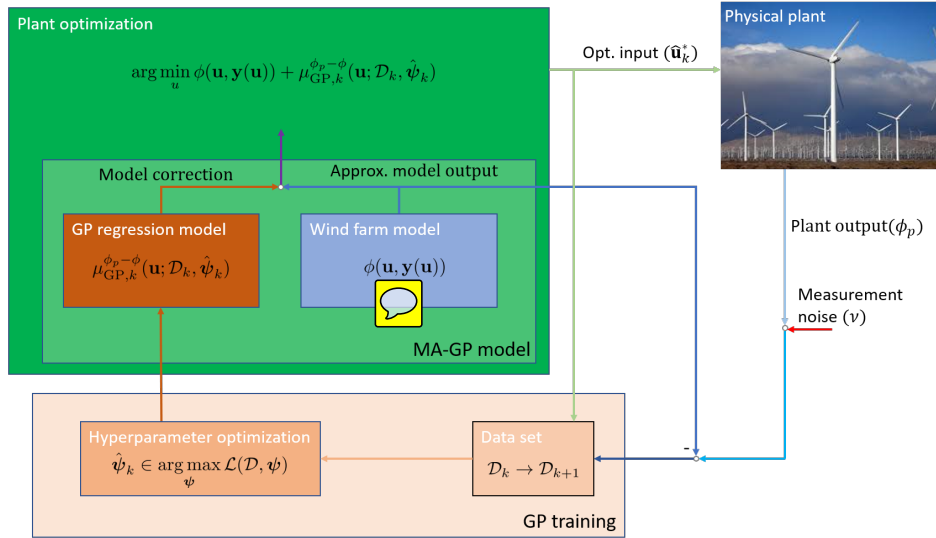


Figure 1. The basic idea of the MA-GP scheme for a wind farm. The GP regression model creates an input-output map of the control inputs to the plant-model mismatch. In the MA-GP model the GP regression model is used to correct the output of the approximate model. This MA-GP model is used in the optimization to compute optimal control inputs for the wind farm. The inputs and the difference between the measured and estimated output of plant and model, respectively, are used to update the data set \mathcal{D} and the hyperparameter ψ . The measured outputs of the plant are corrupted by **noise**¹

Algorithm 1: Basic MA-GP scheme (del Rio Chanona et al., 2019)

Initialisation: GP regression model $\mu_{\text{GP}}^{\phi_p - \phi}$ and hyperparameters $\hat{\psi}_0$ found with (9) and data set \mathcal{D}_0 ; Optimal operation point of the approximate model \mathbf{u}_0 .

for $k = 0, 1, \dots$ **do**

- Solve modified optimization problem Eq. (13);
- Filter new operating point \mathbf{u}_{k+1} with Eq. (5);
- Evaluate approximate model at new operating point \mathbf{u}_{k+1} ;
- Obtain measurements of cost function $\phi_p(\mathbf{u}_{k+1})$;
- Update the data set \mathcal{D}_{k+1} with input \mathbf{u}_{k+1} and output $y_{k+1} = \phi_p(\mathbf{u}_{k+1}) - \phi(\mathbf{u}_{k+1}) + \nu_{k+1}$;

if *HypOpt* **then**

Update hyperparameters $\hat{\psi}_{k+1}$ with new data set \mathcal{D}_{k+1} and Eq. (9);

end

Update GP regression term $\mu_{\text{GP}}^{\phi_p - \phi}$ using \mathcal{D}_{k+1} and hyperparameters $\hat{\psi}_{k+1}$;

end





3.2 Numerical turbine and wake models

The wind turbines in the wind farm are represented using the actuator disc theory, which couples the power and thrust coefficient, C_P and C_T (Burton et al., 2011)

$$C_P = 4a(1 - a)^2, \quad (14)$$

$$C_T = 4a(1 - a), \quad (15)$$

where a is the axial induction factor. The axial induction factor indicates the ratio of wind velocity reduction at the turbine disk compared to the upstream wind velocity. The steady-state power of each turbine under yaw misalignment is given by (Gebraad et al., 2016)

$$P = \frac{1}{2} \rho A C_P \cos \gamma^p u^3, \quad (16)$$

where A is the rotor area, ρ the air density and p a correction factor. In actuator disc theory $p = 3$ (Burton et al., 2011). However, based on large-eddy simulations, the turbine power yaw misalignment has been shown to match the output when $p = 1.88$ for the NREL 5MW turbine (Annoni et al., 2018), which we will use in this article. In the numerical study it will be important to implement a "plant" and model, which are different from each other. Therefore, a second adjusted actuator disk turbine model is created. The FLORIS toolbox (NREL, 2019) contains a table with wind velocities and corresponding thrust and power coefficients of the NREL 5MW turbine. These data are fitted to a new model based on the actuator disk model. The equation for the thrust coefficient C_T is given by Eq. (15) while for the power coefficient C_P three new parameter are identified resulting in

$$C_P = 7.037a(0.625 - a)^{1.364}. \quad (17)$$

The model fit is visualised in Fig. 2. Important in the numerical example is the different connection between thrust and power coefficients of both models (Fig. 2b). For the turbine dimensions the NREL 5-MW wind turbine is used (Jonkman et al., 2009). Consequently, the rotor diameter is $D = 136 \text{ m}$ and the hub height $H_H = 90 \text{ m}$.

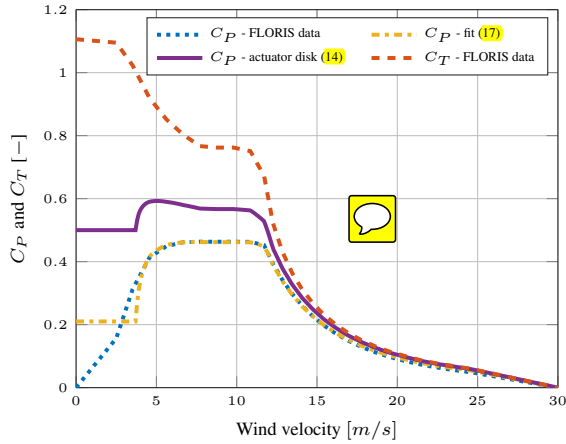
The Gaussian wake model by Bastankhah and Porté-Agel (2014, 2016) is used to model the flow in the wind farm. The three-dimensional steady-state far wake velocity is assumed to be Gaussian distributed and can be estimated with

$$\frac{\bar{v}(x, y, z)}{\bar{v}_\infty} = 1 - C e^{-0.5((y-\delta)/\sigma_y)^2} e^{-0.5((z-z_h)/\sigma_z)^2}, \quad (18a)$$

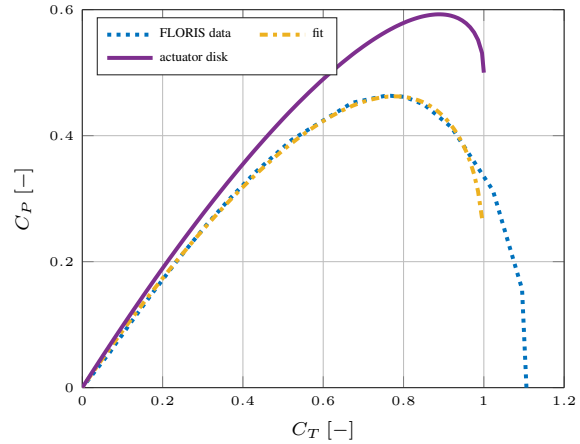
$$C = 1 - \sqrt{1 - \frac{C_T \cos \gamma}{8(\sigma_y \sigma_z / d^2)}}, \quad (18b)$$

where z_h is the tower height, δ is the wake deflection, and σ_y and σ_z are the wake widths in lateral and vertical directions. An important variable for the model is the skew angle of the flow past a yawed turbine. The flow skew angle is approximated by

$$\theta \approx \frac{\alpha_1 \gamma}{\cos \gamma} \left(1 - \sqrt{1 - C_T \cos \gamma} \right), \quad (19)$$



(a) Comparison of C_P values in dependency of the wind velocity. The dashed line gives the corresponding thrust coefficient, which is the same for both models.



(b) $C_P - C_T$ curve of the data and both models.

Figure 2. Comparison between data, the new model based on the actuator disk model and the actuator disk model. The thrust coefficients are kept smaller than one for the actuator disk models. The models give a different connection between thrust and power coefficients.

where α_1 is a parameter. Bastankhah and Porté-Agel (2016) use $\alpha_1 = 0.3$ and NREL (2019) uses $\alpha_1 = 0.6$ to better fit high-fidelity observations. In the simulation study different values are chosen for α_1 parameter in the plant and approximated model resulting in different optimal operating points.

4 Numerical case study

175 In this section numerical results of the MA-GP approach are presented. The control inputs of the wind farms are the yaw angles γ_i and the thrust coefficients $C_{T,i}$ of each turbine. Hence, the wind farm has $2N$ control inputs, where N is the amount of wind turbines. The objective of the optimization is to maximize the power production $P_{tot} = \sum_i P_i$ of the wind farm. The control inputs are constrained by box constraints with

$$0 \leq C_{T,i} \leq 0.95, \text{ and } 0^\circ \leq \gamma_i \leq 40^\circ. \quad (20)$$

180 In the MA-GP approach only measurements of the total power output of the wind farm are used. The hyperparameter optimization is performed using the MATLAB optimization toolbox and the nonlinear programming solver *fmincon*. For the optimization of the control inputs of the wind farm the open source software tool *CasADi* (Andersson et al., 2019) is used. *CasADi* is a symbolic framework that provides gradients using Algorithmic Differentiation. The software package *Ipopt* is used as a solver for the nonlinear program (Wächter and Biegler, 2006).

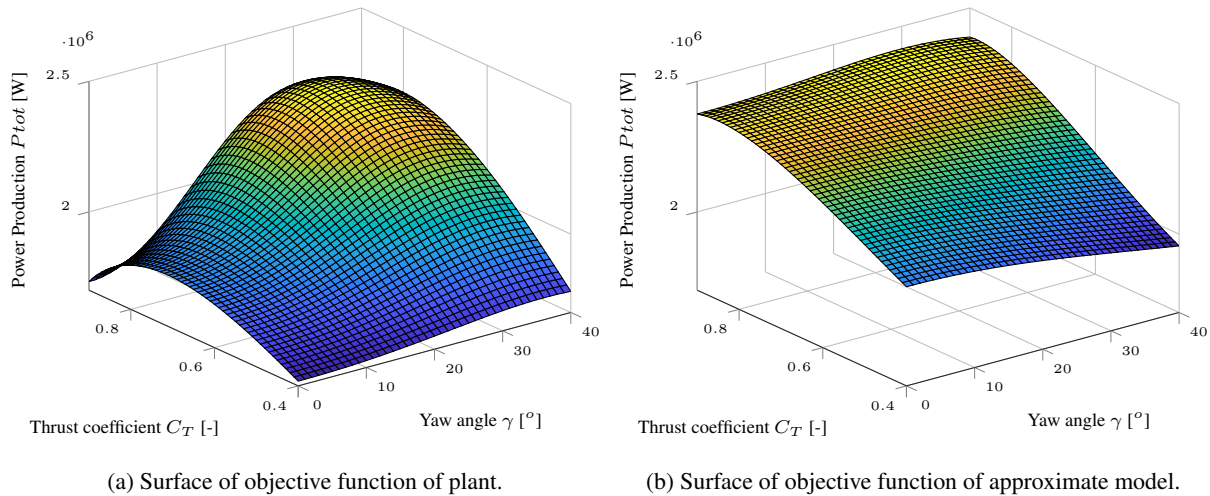


Figure 3. The power production of plant and approximate model in dependency of the control inputs of the upwind turbine.

185 4.1 Two turbine case



The operating points of two turbines in a row are optimized. The thrust and yaw angle of the downwind turbine are fixed resulting in only two optimization variables in the MA-GP approach. The downwind turbine is operated at its greedy operation point. The turbine row is facing the wind and the spacing between turbines is 5D. The power production of the wind farm in dependency of the control inputs of the upwind turbine is shown in Fig. 3. The optimal operation point of the plant is
 190 $C_{T,p} = 0.82$ and $\gamma_p = 31^\circ$ and of the approximate model $C_{T,p} = 0.89$ and $\gamma_p = 29^\circ$. Indeed, the relative optimization error of the model is only 1.67%. Still, the model assume that the power production is much less sensitive to changes in the yaw angle, which should be corrected by the MA-GP approach.

Four training points at $C_T = [0.4, 0.8]^T$ and $\gamma = [0^\circ, 25^\circ]^T$ are used to create the initial training set of the GP regression model. The power production of the corrected model in dependency of the control inputs is shown in Fig. 4a. The contour plot of the
 195 objective function of the plant, approximate model and MA-GP model after the initial training is shown in Fig. 4b. Clearly four operating points are not sufficient to correct the approximate model correctly. In fact, the optimal operating point of the MA-GP model has an error of 2.87%, which is larger than the original error of the approximate model.

The MA-GP approach is initialised at the optimal operating point of the approximate model. In each iteration the hyper-parameters and the data set of the GP regression model are updated. The new operating point is filtered with Eq. (5) and
 200 $\mathbf{L} = \text{diag}(0.4, 0.4)$. The MA-GP approach is able to correct the approximate model and drive the process to its optimal operating point. Fig 5 shows the operating points of the first ten iterations. After four iterations the error in power production is about 0.2% and after ten iterations it is 0.0009%. In addition, the contour lines of the objective function are well approximated. A larger difference between MA-GP model and the plant can be observed at the edges away from the current operating points. Data points at the edges are necessary to improve the identification there. However, to drive the process to its optimal operating
 205 points a correct identification of the objective function far away from the maximum is unnecessary. Clearly the initial training

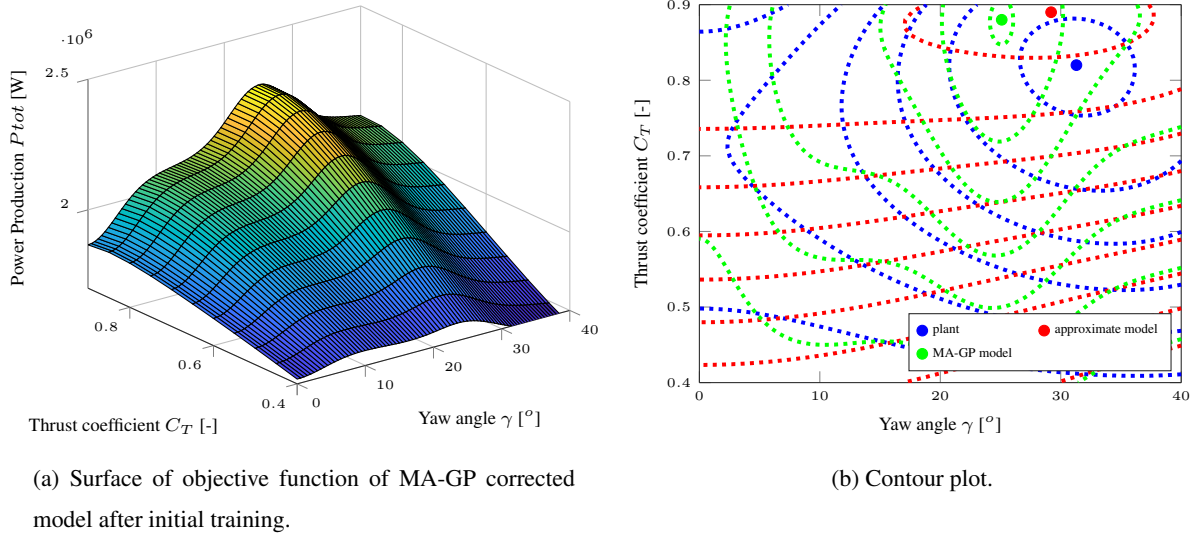


Figure 4. The power production of MA-GP model in dependency of the control inputs of the upwind turbine and the contour plot of plant, approximate model and MA-GP model after the initial training.

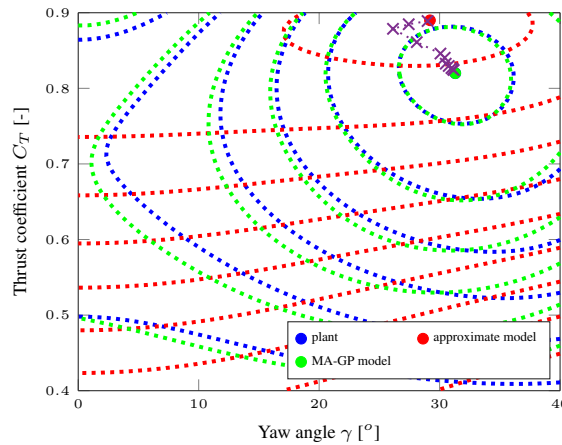


Figure 5. The contour plot of plant, approximate model and MA-GP model after ten iterations. The operating points of each iteration are marked with a cross.

set with only four operating points could be increased to improve the identification of the initial model of the MA-GP approach.

In the current example it is assumed that the measurements are noise-free. If noise is added to the power measurements the correct identification becomes more challenging and a larger training data set is necessary. A noise with a standard deviation of 50 kW is added to the measurement. The standard deviation is of the same size as the error in the power production of approximate model and plant at the optimal operating point. A training data set of 20 points is created. After ten iterations the error in the power production is about 0.6 %. The algorithm is able to converge. However, due to the measurement noise a

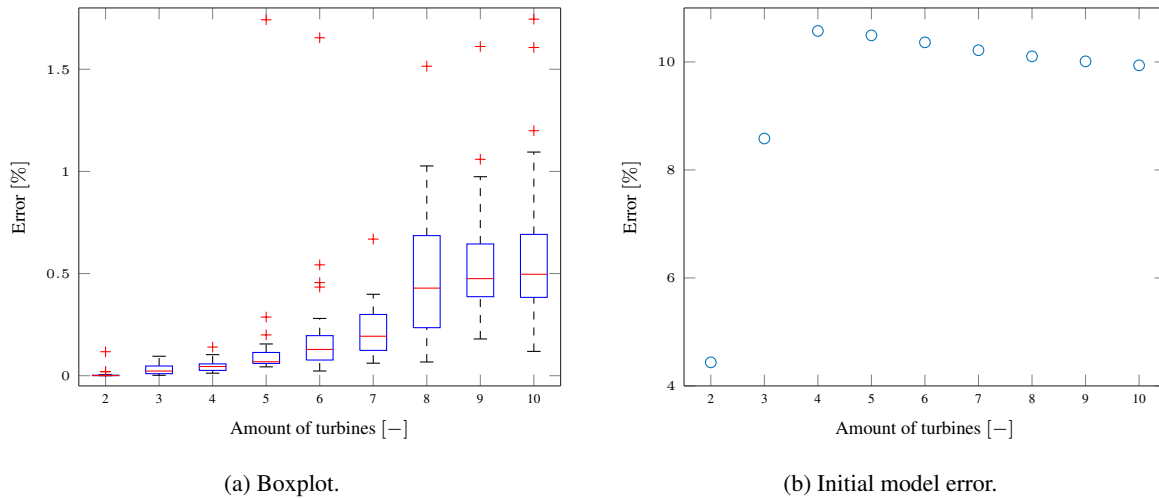


Figure 6. The boxplot of the optimization results for the differently long wind turbine rows on the left. The red line indicates the median. The bottom and top edges of the blue box indicate the 25th and 75th percentiles, respectively. The red marker indicate outliers and the whiskers extend to the most extreme data points not considered as outliers. The error of the MA-GP approach and the initial error dependent of the amount of turbines in the row. The initial error in the model depending on the amount of turbines in the row on the right.

small error remains after ten iterations. The error can be easily decreased with a larger initial data set, e.g. with a training set of 30 points the error after ten iterations is about 0.35 %.

4.2 n turbine row case

215 In this subsection n turbines aligned in a row are optimized with the MA-GP algorithm. The size of the initial training set is chosen to be $n_d = 10n_u$, where n_u is the amount of control inputs. The operating points of the training set are randomly chosen. The convergence of the MA-GP algorithm is tested on 25 Monte Carlo simulations. The difference between each run is the initial training set.

220 The statistic of the error after 25 iterations is shown in Fig. 6a. The error increases with the amount of turbines while it is almost zero for 2 to 4 turbines. Even though, the error increases with the amount of turbines the algorithm is able to reduce the model error significantly (Fig. 6b). It is not surprising that the error increases with the amount of control inputs. The control inputs are mapped to the total power output of the wind farm. With a large amount of control inputs the correct identification of this input-output map becomes more challenging, which increases the error in the MA-GP algorithm. Again, the error could be decreased with more data in the training set. Currently, the optimization of the process and the optimization of the hyperparameters takes less than a second even for the ten turbine case. Consequently, it is possible to increase the data set. However, the computational time of the GP regression grows cubic with the amount of data. Therefore, at some point a trade-off between performance and computational time is necessary.

In contrast to purely model-free approaches, e.g. extremum seeking (Johnson and Fritsch, 2012) or MPPT (Gebraad et al.,

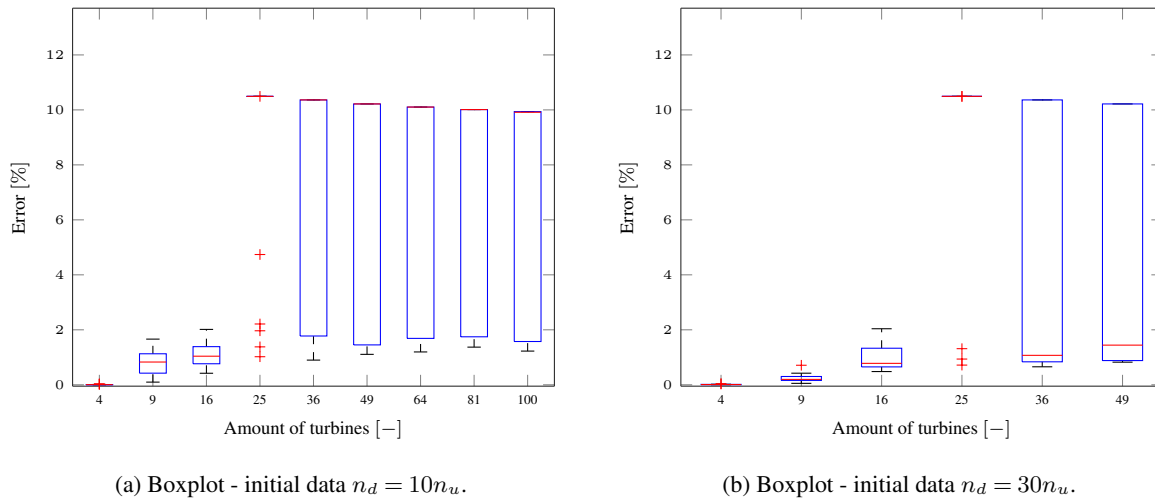


Figure 7. The boxplot of the optimization results for the differently large wind turbine grids. The red line indicates the median. The bottom and top edges of the blue box indicate the 25th and 75th percentiles, respectively. The red marker indicate outliers and the whiskers extend to the most extreme data points not considered as outliers. The error of the MA-GP approach and the initial error dependent of the amount of turbines in the row. The difference between both runs is the size of the initial training set.

2013), is the MA-GP the algorithm able to find a near optimal point in one iteration. The MA-GP model is already a better representation of the plant after the initial training than the approximate model. Nonetheless, measurements close to the optimum can help to refine the MA-GP model.

4.3 $n \times n$ turbine grid case

In this subsection the turbines in the wind farm are arranged in a $n \times n$ grid. The wind direction is aligned with the rows of the grid. Interaction between parallel rows is neglectable. Consequently, the wind farm consists of n turbine rows each containing n turbines. The distance between turbines is $5D$. The identification of the power production of this wind farm layout becomes more challenging. The input space increased and the sensitivity of inputs onto the total power production of the wind farm become similar.

Again the size of the initial training set is chosen to depend linearly on the size of the amount of control inputs with $n_d = 10n_u$. Otherwise the setup is the same as in the turbine row case.

240 The error after 25 iterations is shown in Fig. 7a. Again the algorithm converges for a small amount of turbines. However, the error in the optimization increases as the amount of turbine increase. Moreover, for grids with 25 and more turbines the majority of the optimizations get stuck at the initial conditions, which is defined by the optimal operation point of the model (Fig. 6b)². Moreover, even in the cases where the MA-GP improves the performance of the wind farm the algorithm converges to errors in the range of 1% to 2% after 25 iterations. These are much larger than observed in the turbine row case.

²The percentage in initial error of the turbine row is equal to the percentage in initial error of the grid.



245 The problems to identify the plant model correctly with a larger inputs space are not surprising. The sample density decreases drastically for larger inputs spaces. The size of the initial training set is increased linearly while it would have to increase exponentially to preserve the same sampling density. For the wind farm with 100 wind turbines and the current setup the hyperparameter optimization takes usually about 15 s. **In some rare cases it took about 5 min.** The plant optimization takes less than 10 s. Consequently, the initial data set could be increased to improve the performance of the larger wind farms.

250 The increase of the initial training set improves the convergence of the method for both small and large inputs spaces (Fig. 7b). Nevertheless, even with the larger size of the initial training set it is challenging to converge to the correct optimum point for cases with a large input space. A larger training set would be necessary for these cases. On the other hand, it also has to be pointed out that the training of the hyperparameters in the GP regression scales cubic with the amount of data. Obviously this limits the size of the initial training set. **Otherwise the approach becomes quickly computational infeasible.** In

255 case of an initial set of $n_d = 10n_u$ and a wind farm with 49 turbines the median time for the hyperparameter optimization is about 3 s. The maximum computational time in the 625 hyperparameter optimization is about 60 s. In case of an initial set of $n_d = 30n_u$ the median optimization time is about 50 s while the maximum optimization time is about 23 min. In these cases the optimization algorithm did not converge to an optimum and the maximum amount of iterations until termination was performed. The optimization time could be reduced by limiting the number of iterations. It is expected that it will not influence
260 the performance since the objective function value in cases the optimization did not converge to an optimum did not change for most of the iterations.

If the MA-GP algorithm for the larger wind farms converges to an optimum it usually takes first a few iterations, where the wind farm is operated at the model optimum point, before the error reduction begins. Obviously the algorithm needs the additional information around the operating point. Interestingly, once the algorithm actually left the initial operating point it converges
265 relatively quickly to an **operating point close to the actual optimum.** This is a strong indication that exploration or even just small excitation around an operating point should be activated if the operating point does not change for some time.

Nonetheless, the results show clearly that the MA-GP is able to improve the performance of the model-based optimization for some of the cases. It is not clear how the initial data sets differ for these successful cases. However, it is expected that a large amount of operation points can be excluded from the initial training set of the GP regression **since it is known from the**
270 **model that they are far away from the optimum operating point.** Currently, the initial training set is chosen randomly by Latin hypercube sampling. A smarter selection with a larger density of points around the optimal operating point of the model may improve the MA-GP approach without increasing the initial data set.

5 Conclusions

The modifier-adaptation approach with Gaussian processes applied to wind farm control is presented. It is a real-time optimization strategy, which corrects optimization model errors by using plant measurements. In the wind farm case the total power
275 production is assumed to be measured and used in the MA-GP approach. **The approach works exceptionally well** for small input spaces. Here the GP regression is able to correct the model almost perfectly. Consequently, operating points very close



to the real optimum are found in the optimization. For larger input spaces, on the other hand, the error increases. Moreover, for the grid-type wind farm layout with more than 25 turbines convergence with the relatively small initial training sets used in
280 this work could not be achieved at all times.

In future work the performance of the method for large inputs spaces has to be improved. Several ideas are possible to achieve it:

- Increase the training set until it becomes computational unfeasible to increase the training set further.
- Choose the training data points **in a smarter way** such that they provide enough information about the regions around the
285 expected optimum.
- Extend the algorithm with an exploration part. This can be achieved, for example, by including the variance of the GP regression model in the optimization.
- Include the single turbine power measurements in the identification of the GP regression model. In such a multi-input and multi-output approach the sensitivities of control inputs to the single outputs increase. The model identification should
290 benefit from the approach. Moreover, it is expected that a smaller data set is necessary to achieve the same performance as with the in the article presented multi-inputs and single-output approach. The idea is pursued in Andersson et al. (2020a) with very promising results in increasing the accuracy of the approach with a smaller initial data set.

In addition, the sensitivity of the approach to measurements and inputs noise has to be investigated. In Andersson et al. (2020b) a simple way how to include input noise explicitly in the MA-GP approach is presented. **Finally, the model identification should
295 be tested on high fidelity and real data. A preliminary study on a nine turbine wind farm case using data from the high-fidelity simulator SOWFA (Churchfield et al., 2012) will be presented in Andersson et al. (2020c).**

Author contributions. LEA compiled the literature review, performed numerical simulations, post-processed the data, and wrote the article. LI helped formulate the methodology used in the article and participated in structuring and reviewing of the article.

Competing interests. The authors declare that they have no conflict of interest.

300 *Acknowledgements.* This work was supported by OPWIND, RCN project no. 268044.



References

- Adaramola, M. and Krogstad, P.-Å.: Experimental investigation of wake effects on wind turbine performance, *Renewable Energy*, 36, 2078–2086, 2011.
- Andersson, J. A. E., Gillis, J., Horn, G., Rawlings, J. B., and Diehl, M.: CasADi – A software framework for nonlinear optimization and
305 optimal control, *Mathematical Programming Computation*, 11, 1–36, <https://doi.org/10.1007/s12532-018-0139-4>, 2019.
- Andersson, L. E., Bradford, E. C., and Imsland, L.: Distributed learning and wind farm optimization with Gaussian processes, in: *American Control Conference (ACC), 2020 - [accepted]*, 2020a.
- Andersson, L. E., Bradford, E. C., and Imsland, L.: Gaussian processes modifier adaptation with uncertain inputs using distributed learning and optimization on a wind farm, in: *IFAC World congress 2020 - [submitted]*, 2020b.
- 310 Andersson, L. E., Doekemeijer, B., van der Hoek, D., and Imsland, L.: Adaptation of Engineering Wake Models using Gaussian Process Regression and High-Fidelity Simulation Data, in: *TORQUE 2020 - [submitted]*, 2020c.
- Annoni, J., Seiler, P., Johnson, K., Fleming, P., and Gebraad, P.: Evaluating wake models for wind farm control, in: *2014 American Control Conference*, pp. 2517–2523, <https://doi.org/10.1109/ACC.2014.6858970>, 2014.
- Annoni, J., Gebraad, P. M., Scholbrock, A. K., Fleming, P. A., and Wingerden, J.-W. v.: Analysis of axial-induction-based wind plant control
315 using an engineering and a high-order wind plant model, *Wind Energy*, 19, 1135–1150, 2016.
- Annoni, J., Fleming, P., Scholbrock, A., Roadman, J., Dana, S., Adcock, C., Porte-Agel, F., Raach, S., Haizmann, F., and Schlipf, D.: Analysis of control-oriented wake modeling tools using lidar field results, *Wind Energy Science*, 3, 819–831, <https://doi.org/10.5194/wes-3-819-2018>, <https://www.wind-energ-sci.net/3/819/2018/>, 2018.
- Barthelmie, R. J., Hansen, K., Frandsen, S. T., Rathmann, O., Schepers, J., Schlez, W., Phillips, J., Rados, K., Zervos, A., Politis, E., et al.:
320 Modelling and measuring flow and wind turbine wakes in large wind farms offshore, *Wind Energy: An International Journal for Progress and Applications in Wind Power Conversion Technology*, 12, 431–444, 2009.
- Barthelmie, R. J., Hansen, K. S., and Pryor, S. C.: Meteorological controls on wind turbine wakes, *Proceedings of the IEEE*, 101, 1010–1019, 2013.
- Bartl, J. and Sætran, L.: Experimental testing of axial induction based control strategies for wake control and wind farm optimization, in:
325 *Journal of Physics: Conference Series*, vol. 753, p. 032035, IOP Publishing, 2016.
- Bastankhah, M. and Porté-Agel, F.: A new analytical model for wind-turbine wakes, *Renewable Energy*, 70, 116–123, 2014.
- Bastankhah, M. and Porté-Agel, F.: Experimental and theoretical study of wind turbine wakes in yawed conditions, *Journal of Fluid Mechanics*, 806, 506–541, 2016.
- Burton, T., Jenkins, N., Sharpe, D., and Bossanyi, E.: *Wind energy handbook*, John Wiley & Sons, 2011.
- 330 Campagnolo, F., Petrović, V., Bottasso, C. L., and Croce, A.: Wind tunnel testing of wake control strategies, in: *American Control Conference (ACC), 2016*, pp. 513–518, IEEE, 2016.
- Churchfield, M. J., Lee, S., Michalakes, J., and Moriarty, P. J.: A numerical study of the effects of atmospheric and wake turbulence on wind turbine dynamics, *Journal of turbulence*, p. N14, 2012.
- Corten, G. and Schaak, P.: Heat and flux: Increase of wind farm production by reduction of the axial induction, in: *Proceedings of the
335 European Wind Energy Conference*, 2003.
- de Avila Ferreira, T., Shukla, H. A., Faulwasser, T., Jones, C. N., and Bonvin, D.: Real-Time optimization of Uncertain Process Systems via Modifier Adaptation and Gaussian Processes, in: *2018 European Control Conference (ECC)*, pp. 465–470, IEEE, 2018.



- del Rio Chanona, E., Alves Graciano, J., Bradford, E., and B., C.: Modifier-Adaptation Scheme Employing Gaussian Processes and Trust Regions for Real-Time Optimization, in: Proc. of the 12th IFAC Symposium on Dynamics and Control of Process Systems, Florianopolis, Brazil, 2019.
- 340 Fleming, P., Annoni, J., Shah, J. J., Wang, L., Ananthan, S., Zhang, Z., Hutchings, K., Wang, P., Chen, W., and Chen, L.: Field test of wake steering at an offshore wind farm, *Wind Energy Science*, 2, 229–239, 2017.
- Fleming, P., Annoni, J., Churchfield, M., Martinez-Tossas, L. A., Gruchalla, K., Lawson, M., and Moriarty, P.: A simulation study demonstrating the importance of large-scale trailing vortices in wake steering, *Wind Energy Science*, 3, 243–255, <https://doi.org/10.5194/wes-3-243-2018>, <https://www.wind-energ-sci.net/3/243/2018/>, 2018.
- 345 Fleming, P., King, J., Dykes, K., Simley, E., Roadman, J., Scholbrock, A., Murphy, P., Lundquist, J. K., Moriarty, P., Fleming, K., van Dam, J., Bay, C., Mudafort, R., Lopez, H., Skopek, J., Scott, M., Ryan, B., Guernsey, C., and Brake, D.: Initial results from a field campaign of wake steering applied at a commercial wind farm – Part 1, *Wind Energy Science*, 4, 273–285, <https://doi.org/10.5194/wes-4-273-2019>, <https://www.wind-energ-sci.net/4/273/2019/>, 2019.
- 350 Gebraad, P., Teeuwisse, F., Van Wingerden, J., Fleming, P. A., Ruben, S., Marden, J., and Pao, L.: Wind plant power optimization through yaw control using a parametric model for wake effects – a CFD simulation study, *Wind Energy*, 19, 95–114, 2016.
- Gebraad, P. M. and Van Wingerden, J.: A control-oriented dynamic model for wakes in wind plants, in: *Journal of Physics: Conference Series*, vol. 524, p. 012186, IOP Publishing, 2014.
- Gebraad, P. M., van Dam, F. C., and van Wingerden, J.-W.: A model-free distributed approach for wind plant control, in: *American Control Conference (ACC)*, 2013, pp. 628–633, IEEE, 2013.
- 355 Horvat, T., Spudić, V., and Baotić, M.: Quasi-stationary optimal control for wind farm with closely spaced turbines, in: *MIPRO, 2012 Proceedings of the 35th International Convention*, pp. 829–834, IEEE, 2012.
- Howland, M. F., Lele, S. K., and Dabiri, J. O.: Wind farm power optimization through wake steering, *Proceedings of the National Academy of Sciences*, 116, 14 495–14 500, 2019.
- 360 Jensen, N. O.: A note on wind generator interaction, 1983.
- Jiménez, Á., Crespo, A., and Migoya, E.: Application of a LES technique to characterize the wake deflection of a wind turbine in yaw, *Wind energy*, 13, 559–572, 2010.
- Johnson, K. E. and Fritsch, G.: Assessment of extremum seeking control for wind farm energy production, *Wind Engineering*, 36, 701–715, 2012.
- 365 Johnson, K. E. and Thomas, N.: Wind farm control: Addressing the aerodynamic interaction among wind turbines, in: *American Control Conference*, 2009. ACC'09., pp. 2104–2109, IEEE, 2009.
- Jonkman, J., Butterfield, S., Musial, W., and Scott, G.: Definition of a 5-MW reference wind turbine for offshore system development, National Renewable Energy Laboratory, Golden, CO, Technical Report No. NREL/TP-500-38060, 2009.
- Katic, I., Højstrup, J., and Jensen, N. O.: A simple model for cluster efficiency, in: *European wind energy association conference and exhibition*, 1987.
- 370 Marchetti, A., Chachuat, B., and Bonvin, D.: Modifier-adaptation methodology for real-time optimization, *Industrial & engineering chemistry research*, 48, 6022–6033, 2009.
- Marchetti, A. G., François, G., Faulwasser, T., and Bonvin, D.: Modifier Adaptation for Real-Time Optimization – Methods and Applications, *Processes*, 4, 55, 2016.
- 375 Medici, D.: Experimental studies of wind turbine wakes: power optimisation and meandering, Ph.D. thesis, KTH, 2005.



- Munters, W. and Meyers, J.: Effect of wind turbine response time on optimal dynamic induction control of wind farms, in: *Journal of Physics: Conference Series*, vol. 753, p. 052007, IOP Publishing, 2016.
- NREL: FLORIS. Version 1.0.0, <https://github.com/NREL/floris>, 2019.
- 380 Park, J., Kwon, S., and Law, K. H.: Wind farm power maximization based on a cooperative static game approach, in: *Active and Passive Smart Structures and Integrated Systems 2013*, vol. 8688, p. 86880R, International Society for Optics and Photonics, 2013.
- Rasmussen, C. E. and Williams, C. K.: *Gaussian processes for machine learning*, the MIT Press, 2, 4, 2006.
- Rotea, M. A.: Dynamic programming framework for wind power maximization, *IFAC Proceedings Volumes*, 47, 3639–3644, 2014.
- Schepers, J. and Van der Pijl, S.: Improved modelling of wake aerodynamics and assessment of new farm control strategies, in: *Journal of Physics: Conference Series*, vol. 75, p. 012039, IOP Publishing, 2007.
- 385 Snelson, E. and Ghahramani, Z.: Sparse Gaussian processes using pseudo-inputs, in: *Advances in neural information processing systems*, pp. 1257–1264, 2006.
- Steinbuch, M., De Boer, W., Bosgra, O., Peeters, S., and Ploeg, J.: Optimal control of wind power plants, *Journal of Wind Engineering and Industrial Aerodynamics*, 27, 237–246, 1988.
- 390 Veers, P., Dykes, K., Lantz, E., Barth, S., Bottasso, C. L., Carlson, O., Clifton, A., Green, J., Green, P., Holttinen, H., Laird, D., Lehtomäki, V., Lundquist, J. K., Manwell, J., Marquis, M., Meneveau, C., Moriarty, P., Munduate, X., Muskulus, M., Naughton, J., Pao, L., Paquette, J., Peinke, J., Robertson, A., Sanz Rodrigo, J., Sempreviva, A. M., Smith, J. C., Tuohy, A., and Wisser, R.: Grand challenges in the science of wind energy, *Science*, 366, <https://doi.org/10.1126/science.aau2027>, <https://science.sciencemag.org/content/366/6464/eaau2027>, 2019.
- Wächter, A. and Biegler, L. T.: On the implementation of an interior-point filter line-search algorithm for large-scale nonlinear programming, *Mathematical Programming*, 106, 25–57, <https://doi.org/10.1007/s10107-004-0559-y>, <http://dx.doi.org/10.1007/s10107-004-0559-y>, 2006.
- 395 Wagenaar, J., Machielse, L., and Schepers, J.: Controlling wind in ECN’s scaled wind farm, *Proc. Europe Premier Wind Energy Event*, pp. 685–694, 2012.